# THE LUND MODEL, MULTIPLE SCATTERING, AND FINAL STATES*

Gösta Gustafson

Lund University
Box 117, 221 00 Lund, Sweden

*(Received May 12, 2008)*

In this talk I present a short review of string hadronization, parton cascades, multiple scattering, final states, and underlying events.

PACS numbers: 12.38.Cy, 12.38.Lg, 13.60.–r, 13.85.–t

## 1. Introduction

In $e^+e^-$ annihilation the total cross-section is determined by the electroweak interaction, while the strong interaction only is responsible for a small correction of relative magnitude $\alpha_s/\pi$. To describe the final states it is, however, necessary to include both the development of the initial perturbative parton cascade and the subsequent soft hadronization process. At high energies the number of gluons is too large for a description by fixed order matrix elements, which makes it necessary to use approximation schemes and modeling also in this perturbative phase.

For $ep$ scattering and hadronic collisions the situation is much more complicated, as also the total cross-section is affected by the strong interaction, via the initial state gluon radiation. Although these emissions are perturbative and describable by the DGLAP or BFKL evolutions, the input structure functions are non-perturbative, and have to be fitted to experimental data.

At high energy the parton density in the proton becomes very large. In $pp$ or $p\bar{p}$ collisions the unitarity constraint implies that there will be a large number of (semi)hard parton–parton subcollisions in an average $pp$-collision. To gain understanding of the final state properties it is therefore important to have a clear picture of the multiple scattering events. We must also have control over the subsequent final state radiation, the color structure of the partonic state, and the final hadronization process.

* Presented at the School on QCD, Low-$x$ Physics, Saturation and Diffraction, Copanello, Calabria, Italy, July 1–14, 2007.

At HERA there are also indications of multiple collisions and saturation effects in the parton evolution, but the true magnitude of these effects is still under debate.

The outline of these lectures is as follows: Sec. 2 — The soft hadronization, Sec. 3 — Initial and final state parton cascades, Sec. 4 — Multiple scattering, Sec. 5 — Underlying events, Sec. 6 — Theoretical ideas, Sec. 7 — Conclusions.

## 2. Hadronization

In a hard process like $e^+e^-$ annihilation there are two phases, a hard perturbative phase described in terms of quarks and gluons, and a soft non-perturbative phase where the energy of the partons is transformed into hadrons. In a 2-jet event the parton state is a quark–antiquark pair plus possibly some soft or collinear gluons. The hadron distribution is limited in $p_\perp$, and the central region is approximately boost invariant.

In the *Lund String Hadronization model* [1] it is assumed that the confining color field behaves like the magnetic field in a superconductor. In a superconductor of type II the magnetic field is compressed to a stringlike structure, a vortex line, by the electron pair condensate in the groundstate. In the same way we imagine that the color electric field is compressed to a string by the gluon condensate in vacuum. We note that a homogeneous electric or magnetic field is invariant under longitudinal boosts, which implies that a vortexline or string with no transverse motion has a constant energy per unit length, corresponding to a constant force. This string tension for a QCD string is estimated to be about 1 GeV/fm. In the string model we approximate the dynamics of the QCD string by that of the "massless relativistic string", which is a mathematical object with zero transverse extension. As this string cannot be quantized in 3+1 dimensions it must be an approximation, but it seems that the transverse extension of the field plays very little role in the hadronization process.

When a high energy $q\bar{q}$ pair moves apart a string is spanned between them. When the energy in this field is sufficiently large a new $q\bar{q}$ pair can be produced from the energy in the field. The field is canceled in between the new pair, and the string is split in two pieces. This process can be repeated, and the result is two jets of bound $q\bar{q}$ systems. As the field is boost invariant, this is also the case for the produced hadronic system. If the quarks are massless they can be produced in a point and pulled apart. If they have a mass $\mu$ and some transverse momentum $k_\perp$, energy conservation implies that they must classically be produced at a distance $l = \sqrt{\mu^2 + k_\perp^2}/\kappa$, where $\kappa$ denotes the string tension. Such a process can be viewed as a tunneling process, which then gives the factorizing production probability

$$\text{Prob.} \propto \exp\left(-\frac{\pi}{\kappa}\left(\mu^2 + k_\perp^2\right)\right) = \exp\left(-\frac{\pi}{\kappa}\mu^2\right)\exp\left(-\frac{\pi}{\kappa}k_\perp^2\right) . \qquad (1)$$

### *2.1. Hadronization in 1 dimension*

Massless quarks moving in a linear potential in one dimension move along the lightcones. For a bound state formed by a quark and an antiquark moving back and forth in its rest frame in a so called yo-yo mode, the maximal extension is given by $l = E/\kappa$. In a boosted frame the motion along the positive lightcone is extended by a Lorentz factor $\gamma$, while the motion along the negative lightcone is shortened by a factor $1/\gamma$, which leaves the area spanned by the string in one period invariant.

The motion of a high energy pair $q_0$ and $\bar{q}_0$ is shown in Fig. 1. The string breaks repeatedly by the production of new pairs $(q_j, \bar{q}_j)$. The final result is a number of yo-yo systems (mesons) moving away from each other. The separation between any two production points is spacelike, and therefore there is no time ordering for the production points. The result is boost-invariant, and in another Lorentz frame it is not the meson formed by the pair $(q_j, \bar{q}_{j-1})$, which is produced first in time. We also note that the hadrons can be ordered in "rank", where two successive hadrons share the quark and antiquark from a common breakup. This ordering agrees on average (but not in every individual case) with the ordering in rapidity.

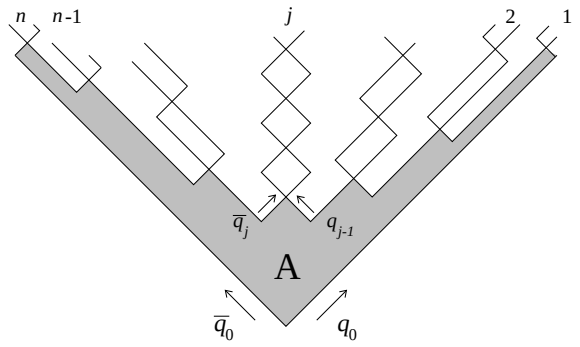


Fig. 1. The hadronization of a high energy $(q_0, \bar{q}_0)$ system. The hadrons can be ordered in "rank", 1, 2, ... $j$, ... $n$. This ordering agrees on average, but not in every case, with the ordering in rapidity.

In the Lund model the probability for a definite final state with $n$ hadrons of mass $m$ is given by the expression

$$P \propto \int\int \left\{\prod_i^n N d^2p_i\, \delta^{(2)}\left(p_i^2 - m^2\right)\right\} \delta^{(2)}\left(\sum_i p_i - P_{\text{tot}}\right) \exp(-bA) . \quad (2)$$

Here $A$ is the color coherent space-time area indicated in Fig. 1 (in units of the string tension $\kappa$), and $b$ is a constant. The expression is a product of a $n$-particle phase-space and an exponential representing a Wilson loop integral, with $bA$ the imaginary part of the action. Thus the model contains two fundamental parameters, $N$ which determines the $n$-particle phase-space, and $b$ which specifies the strength of the string-breaking mechanism.

The simulation of states according to this distribution can be obtained in an iterative way by first determining the momentum of the "last" hadron, meaning the first in rank. When the remaining energy is large this hadron takes a fraction $z$ of the total lightcone momentum $p_+$ given by the distribution

$$\frac{d\,P}{d\,z} = N\frac{(1-z)^a}{z}\exp\left(-\frac{bm^2}{z}\right). \tag{3}$$

This process can be repeated, producing a jet of hadrons. In Eq. (3) the parameters $N$, $b$, and $a$ are related by the normalization constraint $\int dz\, dP/dz = 1$, and the two free parameters can be chosen as $(N, b)$ from Eq. (2) or as $(a, b)$. Combinations of these parameters determine the multiplicity and the correlation between the produced particles. The height of the central plateau is given by the ratio $dn/dy \sim (1+a)/b$, and for fixed multiplicity a larger value for the product $a \cdot b$ corresponds to a more narrow distribution in $z$ or in the difference $y_i - y_{i+1}$, and thus a stronger correlation between the particles.

In real life there are a few extra complications:

1. Different quark species can be produced in the breakup: $u$, $d$, $s$, where the $s$-quark is suppressed by about a factor 3 due to its larger mass.

2. The spins can be combined to give a pseudoscalar particle, a vector meson. Higher spin states are estimated to contribute about 10%.

3. The string can also break by the production of a diquark–antidiquark pair, giving rise to baryons and antibaryons.

4. The distribution in Eq. (3) is only true if the remaining system has a large mass. At the end of the cascade this is no longer true, and the distribution obtained in the MC is not exactly the one determined by the model in Eq. (2). (This has in particular an effect on correlations between the produced hadrons [2].)

Thus besides the two parameters ($a$ and $b$ in Eq. (3)), which determine the gross features of the event, more extra parameters are needed if all details are to be described. The large number of possibilities in each step make analytic calculations impossible. The process is simulated in the `Jetset` MC, which now is incorporated in the `Pythia` package [3].

### *2.2. Gluon jets*

In three dimensions the confining field implies extra degrees of freedom. Any disturbance in the field can only propagate with the speed of light. If one of the particles in a $q\bar{q}$ pair is kicked, this can first be noticed by the partner when it is reached by such a signal, and it must in the meantime continue undisturbed. The energy stored in the field is no longer a function of the distance between the endpoints, but depends on the motion of every point on the string.

It is possible to have transverse excitations on the field. For a reaction $e^+e^- \to q\bar{q}g$ the simplest possibility for the confining field is to have a string stretched between the quark and the gluon, and from the gluon to the antiquark, as indicated in Fig. 2. The string is stretched from the quark to the antiquark via the gluon, and the gluon acts as a transverse excitation on the string. If the transverse extension of the field can be neglected, the dynamics of the confining field can be approximated by the dynamics of the massless relativistic string.

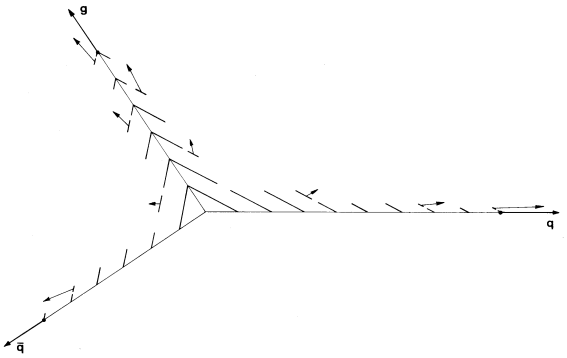


Fig. 2. The space-time development of a quark–antiquark–gluon event. The string is stretched from the quark to the antiquark via the gluon, which moves like a point-like kink carrying energy and momentum. The string breaks by the production of new $q\bar{q}$ pairs, and the final state contains three jets. Soft particles formed in between the jets get a boost by the transverse motion of the string.

The subsequent motion and breakup of the string is also illustrated in Fig. 2. The result is three jets of hadrons in the directions of the three original partons. The transverse motion of the strings gives a boost to the soft particles, which implies that the hadrons are produced around two hyperbolae in momentum space. Thus there are more soft particles between the (anti)quark jet and the gluon jet, than between the quark and antiquark jets. This result can be compared with the hadron distribution in a $e^+e^- \to q\bar{q}\gamma$ event, where the transverse string motion is in the direction opposite

to the photon. Thus there will in this case be an enhancement of particles between the quark and antiquark jets. This "string effect" was first observed by the JADE Collaboration [4] at the PETRA storage ring, and was later also observed at LEP.

Gluon radiation is singular for soft and collinear emissions. A very important feature of the string hadronization model is that it is *infrared stable*. The motion of a soft transverse gluon is soon stopped by the tension in the attached strings. In the subsequent string motion the gluon kink is split into two corners, which do not carry energy or momentum and which are connected by a straight string piece, as shown in Fig. 3(a). The energy in the small sections close to the quark and the antiquark is not sufficient for a hadron, and all breakups will occur in the central string piece, which is stretched and breaks up in the same way as the straight string in Fig. 1. The string motion with a collinear gluon is shown in Fig. 3(b), and also here the effects of the gluon goes to zero in the collinear limit.

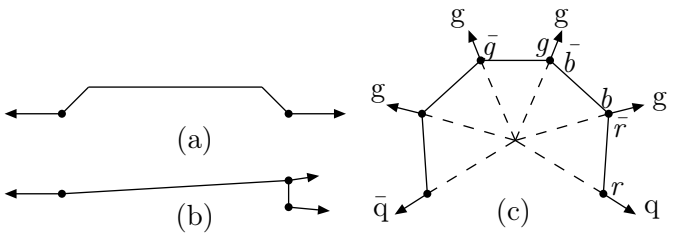


Fig. 3. (a) A soft transverse gluon will soon lose its energy. The kink on the string is split in two corners and a straight string piece is stretched in a way similar to a one-dimensional string. (b) Also for a collinear gluon the energy in the string between the quark and the gluon is too small for a breakup of the string. (c) In a state with many gluons the string is stretched from the quark to the antiquark via the color-ordered gluons, in the figure from red to antired, from blue to antiblue *etc.*

The situation in Fig. 2 can be directly generalized to many gluons. The string is here stretched from the quark via the color-ordered gluons till the antiquark, as shown in Fig. 3(c).

The string hadronization model can be compared to the cluster fragmentation implemented in the `Herwig` MC [5]. In this model the final gluons are split into $q\bar{q}$ pairs, which combine to colorless clusters. The clusters then decay to two hadrons. However, fits to data have brought about some modifications, which also give evidence in favor of stringlike dynamics. Thus high mass clusters are allowed to decay in a stringlike manner, baryon–antibaryon pairs have an angular correlation as if they are pulled apart by the string, and the leading cluster is also not isotropic but oriented in the direction of the string or cluster chain.

## 3. Parton cascades

### *3.1. Timelike cascades*

#### 3.1.1. Single gluon emission

In $e^+e^-$ annihilation the produced high energy quark and antiquark initiate a cascade of gluons. Although very important for the properties of the final states, these emissions have a very small effect on the total hadronic cross-section given by

$$\sigma_{\rm tot} = \sigma_0 \left(1 + \frac{\alpha_{\rm s}}{\pi} + \mathcal{O}\left(\alpha_{\rm s}^2\right)\right) . \tag{4}$$

Here $\sigma_0$ is the 0th order cross-section determined by electroweak dynamics.

The probability for the emission of a single (soft) gluon is given by

$$\frac{dN}{d\,k_\perp^2\,d\,y} \approx \frac{4\alpha_{\rm s}}{3\pi}\frac{d\,k_\perp^2}{k_\perp^2} d\,y\,. \tag{5}$$

The gluon corresponds to dipole emission radiated coherently from the quark and the antiquark forming a *color dipole*. The allowed phase-space is approximately determined by the constraint $|y| < \ln(Q/k_\perp)$, where $Q$ is the cms energy of the virtual photon or $Z$-boson.

The cross-section for 3-jet events diverges for small $k_\perp$, *i.e.* for soft and collinear gluons. This divergence is compensated by virtual corrections to the 2-jet cross-section, thus giving only the small first order correction to the total cross-section in Eq. (4).

The Landau–Pomeranchuk formation time for a gluon is of the order of $1/k_\perp$. This is relatively short for hard emissions and longer for gluons with smaller $k_\perp$. In case of several emissions the transverse momentum can therefore also be interpreted as a time ordering of the gluon emissions. The emission of the "first" gluon, meaning the one with largest $k_\perp$, can then be described with the help of a "Sudakov form factor", $S$, which represents the probability that no gluon is emitted with a larger $k_\perp$:

$$\begin{aligned} \frac{1}{\sigma_0}\,d\sigma_{\rm hardest} &= \frac{4\alpha_{\rm s}}{3\pi}\,\frac{d\,k_\perp^2}{k_\perp^2}\,d\,y \cdot S(k_\perp)\,, \\ S(k_\perp) &= \exp\left(-\int\limits_{k'_\perp > k_\perp} \frac{4\alpha_{\rm s}}{3\pi}\,\frac{d\,k_\perp'^2}{k_\perp'^2}\,d\,y'\right) . \end{aligned} \tag{6}$$

#### 3.1.2. Two gluon emission

If a second gluon is much softer than the first, the emission probability factorizes. The current relevant for the second emission is, however, modified and includes a contribution from the first, harder, gluon. An important property of the emission is due to the interference between opposite color charges. If the first emission produces a red quark, a blue-antired gluon, and an antiblue antiquark, then the red-antired charges radiate coherently as a color dipole formed by the quark and the gluon. In the rest frame of this dipole the distribution is also given by the expression in Eq. (5). In the same way the blue and antiblue charges radiate coherently as a color dipole formed by the gluon and the antiquark. (There is also a color-suppressed term corresponding to a dipole spanned between the quark and the antiquark, with relative weight $-1/N_c^2$.)

In the overall cms the dipoles are boosted with a velocity $v = \cos(\theta/2)$ transversely to the direction of the dipole, where $\theta$ is the opening angle between the motion of the endpoints. The result is a suppression of secondary emissions at larger opening angles. In many applications this coherence effect is approximated by a sharp "angular ordering" cut $\theta' < \theta$ [6].

#### 3.1.3. Dipole cascade model

The result in the previous section can be generalized, and the distribution of a third, still softer, gluon is described by three dipoles. In the large $N_c$ limit all dipoles have different colors, and the gluon emission can be formulated as a *dipole cascade*, where in each step one dipole is split into two dipoles [7]. Each gluon is connected to two dipoles, and the final result is therefore a chain of dipoles. We note that a dipole connects two gluons which in the string hadronization model are connected by a piece of the string. Thus the picture in Fig. 3(c) can also be interpreted as a picture of the dipole cascade, and the color dipole chain joins very nicely onto the string in the subsequent hadronization process. The evolution of this dipole cascade is simulated in the `Ariadne` MC event generator [8], and the results agree with data from LEP and PETRA to a very high accuracy (see *e.g.* Ref. [9]).

Expressed in parton degrees of freedom a dipole split corresponds to a $2 \to 3$ transition, taking into account the coherence between the color and anticolor of the two parent partons. In the alternative formulations of the cascade implemented in `Herwig` [5] and `Pythia` [3] this coherence is instead taken into account by the angular ordering constraint described above.

The factorizing result described here is correct in the large $N_c$ limit, and for strongly ordered emissions. In reality the emissions are not strongly ordered. Harder gluons are not uncommon, and they have in addition a very

strong effect on the properties of the final state. Some non-leading effects are taken into account by including the non-singular corrections to the dipole splitting in Eq. (5) (and the corresponding terms in a gluon–gluon dipole). The hardest gluon is particular important, and it is therefore essential to have this generated in accordance with the exact perturbative matrix element. In view of these problems it may be surprising that the models are so very successful in reproducing the experimental data. There are also many studies of color-suppressed effects proportional to $1/N_c^2$, which could *e.g.* give color singlet gluon systems which hadronize separated from the remainder. So far such effects appear to be small, and have not been confirmed experimentally.

#### 3.1.4. Final state

The evolution of the parton cascade is illustrated in Fig. 4. The triangle in Fig. 4(a) represents the phase-space for the first gluon given by $|y| < \ln(Q/k_\perp)$. If the first gluon is determined by $k_{\perp 1}$ and $y_1$ the phase-space for the second gluon is increased. This increase is represented by the extra fold in Fig. 4(b). In the same way each emission adds a fold to the phase-space for the later (softer) gluons, and the final result is the multifaceted surface in Fig. 4(c). This surface has a fractal structure; when studied with increased resolution more gluons are resolved. The hadron multiplicity is related to the length of the baseline, which for running coupling grows like $\exp(2\sqrt{\alpha_0 \ln Q^2}\,)$, where $3\alpha_s(Q^2)/2\pi \equiv \alpha_0/\ln Q^2$.

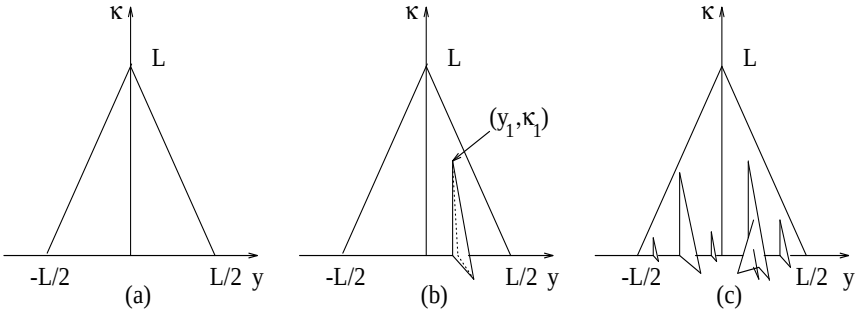


Fig. 4. (a) The phase-space for gluon emission in $e^+e^-$ annihilation is a triangular region in the $(y, \kappa \equiv \ln k_\perp^2)$-plane. The height of the triangle is given by $L = \ln s$. (b) When one gluon is emitted at $(y_1, \kappa_1)$ the phase-space for a second (softer) gluon is represented by the area of this folded surface. (c) Each emitted gluon increases the phase-space for softer gluons. The total phase-space is represented by this multifaceted surface.

This picture can be compared with the evolution in the `Herwig` MC. Here the emissions are ordered in angle or rapidity, which means that the area in Fig. 4(c) is covered "sideways". Thus a soft gluon is often emitted before a harder one, and the most important difference between the two formalisms is caused by the effect of the recoils.

### *3.2. Spacelike cascades*

In a high energy *ep* or *pp* collision the initial partons in a target proton develop similar parton cascades. A projectile can interact with any of the partons in the cascade, which implies that the total cross-section grows with increasing collision energy. This implies that we have here two separate problems: the total cross-section and the properties of the final states. Note that the partons in the cascades have spacelike momenta, and only those branches which interact with the projectile can come on shell and produce real final state particles. A second complication is that the process depends on two separate variables, $Q^2$ and $W^2$, while in $e^+e^-$ annihilation we have only one scale $Q^2$.

#### 3.2.1. Cross-section

For *large* $Q^2$ $k_\perp$-ordered emissions dominate, and the variation of the structure functions is determined by DGLAP evolution.

For *small* $x$ *and limited* $Q^2$, in the BFKL regime, also $k_\perp$-non-ordered emissions are important.

A formalism which interpolates between the DGLAP and BFKL regimes was presented by Catani, Ciafaloni, Fiorani, and Marchesini, the CCFM model [10]. This was reformulated and generalized in the *Linked Dipole Chain* model, LDC [11]. The result is here that those initial state radiation chains which have monotonously increasing $k_\perp$ have the same weight as in DGLAP. However, links in the initial radiation ladder where $k_\perp$ is decreasing are not excluded, but suppressed by a factor $\min(1, k^2_{\perp i}/k^2_{\perp i-1})$.

With a running coupling $\alpha_s$, ladder rungs with small $k_\perp$ are favored. For small $x$ the dominating chains therefore first have a non-ordered BFKL-type region with small $k_\perp$, followed by an ordered DGLAP evolution, with virtualities up towards $Q^2$. This implies also that the structure functions can be well fitted by DGLAP evolution, if the soft input for small $Q^2$ has a tail down to small $x$.

#### 3.2.2. Final state properties

To find the final state, knowing what branch(es) interacted with the projectile, we must first isolate the branches in the cascade leading to the interacting twig, and after that add final state radiation in appropriate parts

of phase-space. The separation between initial and final state radiation depends on the formalism, and therefore the regions for final state radiation is model dependent.

The "Soft radiation model", also called the "Color Dipole Model", CDM [12], is a simple heuristic model where all gluons are treated as final state radiation. This model can only describe the final state properties, and not the cross-section. When a quark in a proton is hit by a virtual photon, its color charge separates from the corresponding anticharge in the proton remnant. This separation induces gluon radiation in the same way as the color charge separation in an $e^+e^-$ annihilation event. The most important difference is that the remnant is not pointlike, and therefore the emission of gluons with short wavelengths is suppressed. Although this model has less support from perturbative QCD, it does give the best overall description of the final states observed at HERA. Essential for this result seems to be that the emissions are un-ordered in $k_\perp$, in accordance with BFKL evolution.

## 4. Multiple scattering

### *4.1. Minijet cross-section*

In *collinear factorization* the cross-section for a parton–parton subcollision in proton–proton scattering is given by

$$\frac{d\sigma^{\text{subcoll}}}{dp_\perp^2} \sim \int dx_1 dx_2 f\left(x_1, p_\perp^2\right) f\left(x_2, p_\perp^2\right) \frac{d\hat{\sigma}\left(\hat{s} = x_1 x_2 s, p_\perp^2\right)}{dp_\perp^2}\,. \qquad (7)$$

(Note that one hard subcollision corresponds to 2 jets.) The partonic cross-section $d\hat{\sigma}/dp_\perp^2$ behaves like $1/p_\perp^4$ for small $p_\perp$, which means that a lower cutoff, $p_{\perp\min}$, is needed. The total subcollision cross section is then proportional to $1/p_{\perp\min}^2$, and for $pp$-collisions this cross-section becomes equal to the total cross-section for $p_{\perp\min} \approx 2.5$ GeV at the Tevatron and $\approx 5$ GeV at LHC [13]. Fits to data give $p_{\perp\min} \sim 2$ GeV at the Tevatron and slowly growing with energy [14].

In *$k_\perp$-factorization* there is a dynamic cutoff when the momentum exchange $k_\perp$ is smaller than the virtuality of the two colliding partons, given by $k_{\perp 1}$ and $k_{\perp 2}$ [15]. This approach gives a very similar effect. We conclude that at high energies the subcollision cross-section is much larger than the total inelastic cross-section, which means that on average there must be several hard subcollisions in one event. It was also early suggested that the increase in $\sigma_{\text{tot}}$ is driven by hard parton–parton subcollisions [16, 17].

### *4.2. Experimental evidence for multiple collisions*

#### 4.2.1. Multijet events

Besides from independent multiple subcollisions, multijet events can also originate from multiple bremsstrahlung from two colliding partons. If we study 4-jet events the difference between these two types of events is that in a double parton scattering the four jets balance each other pairwise in the transverse momentum plane, while such a pairwise balance is not present in the multiple bremsstrahlung events. The Axial Field Spectrometer [18] at the ISR proton–proton collider studied an "imbalance parameter" $J = [(\boldsymbol{p}_{\perp 1} + \boldsymbol{p}_{\perp 2})^2 + (\boldsymbol{p}_{\perp 3} + \boldsymbol{p}_{\perp 4})^2]/2$, and found that there is a significant enhancement of events with small values of $J$, which thus showed a clear evidence for multiple subcollisions.

Similar, but less clear, results for 4-jet events have been observed by the CDF [19] and D0 [20] experiments at the Tevatron. A more clear signal for multiple collisions at the Tevatron has instead been seen in events with three jets + $\gamma$ [21]. Evidence for multiple collisions has also been observed in photoproduction by the ZEUS Collaboration [22] at HERA.

#### 4.2.2. Correlations

An important question is whether the hard subcollisions are correlated, or if a high $p_\perp$ event just corresponds to two jets on top of a minimum bias event. If the subcollisions are uncorrelated the probability, $P(n)$, for having $n$ subcollisions should be described by a Poisson distribution. This implies that

$$P(2) = \frac{1}{2} P(1)^2 \,. \tag{8}$$

Here the factor $1/2$ is compensating for double counting. Expressed in the cross-sections $\sigma_n = P(n)\sigma_{\rm nd}$ (where $\sigma_{\rm nd}$ is the inelastic non-diffractive cross-section) this gives the relation $\sigma_2 = \frac{1}{2}\sigma_1^2/\sigma_{\rm nd}$. The experimental groups have used the notation

$$\sigma_2 = \frac{1}{2}\frac{\sigma_1^2}{\sigma_{\rm eff}} \,, \tag{9}$$

which means that $\sigma_{\rm eff} = \sigma_{\rm nd}$ corresponds to uncorrelated subcollisions. The experimental results on 4-jet events referred to above find, however, that $\sigma_{\rm eff}$ is much smaller than $\sigma_{\rm nd}$. Thus at ISR one finds (for jets with $p_\perp > 4$ GeV) $\sigma_{\rm eff} \sim 5$ mb compared to $\sigma_{\rm nd} \sim 30$ mb, CDF finds for 4-jet events ($p_\perp > 25$ GeV) and 3 jets+$\gamma$ the results $\sigma_{\rm eff} \sim 12$ mb and $\sim 14$ mb, respectively, to be compared with $\sigma_{\rm nd} \sim 50$ mb. This means that if there is one subcollision there is an enhanced probability to have also another one. A possible interpretation is that in central collisions there are many hard subcollisions, while there are fewer subcollisions in a peripheral collision.

## 5. Underlying event and minimum bias

### *5.1. Pedestal effect*

The observation that in events with a high $p_\perp$ jet the underlying event is enhanced, the so called *pedestal effect*, is also a sign of correlations between subcollisions. The UA1 Collaboration at the $S\bar{p}pS$ collider studied the $E_\perp$-distribution in $\eta$ around a jet [23]. To avoid the recoiling jet they looked in 180° in azimuth on the same side as the jet. The result is that for jets with $E_\perp > 5$ GeV the background level away from the jet is roughly a factor two above the level in minimum bias events. Similar results have been observed in resolved photoproduction by the H1 Collaboration [24].

### *5.2. CDF analysis and the* `Pythia` *model*

Rick Field has made very extensive studies of the underlying event at the Tevatron (see *e.g.* Ref. [25]). He has here tuned the `Pythia` MC to fit CDF data, and found tunes (*e.g.* tune A and tune DW) which give very good fits to essentially all data. In particular he has looked at the $E_\perp$-flow, the charged particle density, and $p_\perp$-spectra in angular regions perpendicular to a high-$p_\perp$ jet. One noticeable result is that the charged multiplicity in this "transverse" region grows rapidly with the $p_\perp$ of the trigger jet up to $p_\perp(\text{charged jet}) \approx 6$ GeV, and then levels off for higher jet energies at twice the density in minimum bias events. Also the charged particle spectrum has a much higher tail out to large $p_\perp$ in events with a high $p_\perp$ jet, compared to the distribution in minimum bias events. The multiple collisions have a very important effect in the MC simulations, and the data cannot be reproduced if they are not included.

The version of the `Pythia` MC used by Field is an implementation of an early model by Sjöstrand and van Zijl [14]. In this model it is assumed that high energy collisions are dominated by hard parton–parton subcollisions, and also minimum bias events are assumed to have at least one such subcollision. To be able to reproduce the observed 4-jets and the pedestal effect, the parton distribution is assumed to have a more dense central region, described by a sum of two (three-dimensional) Gaussians. For fixed impact parameter, $b$, the number of subcollisions is assumed to be given by a Poisson distribution, with an average proportional to the overlap between the parton distributions in the two colliding protons. Integrated over the impact parameter this gives a distribution which actually can be well approximated by a geometric distribution, that is a distribution with much larger fluctuations than a Poisson.

The `Pythia` model does not include diffraction, and describes only non-diffractive inelastic collisions. Diffraction is related to the fluctuations via the AGK cutting rules [26]. In QCD a single pomeron exchange can be

represented by a gluon ladder. The diagram for double pomeron exchange can be cut through zero, one and two of the exchanged pomerons, with relative weights 1, $-4$, and 2. If we add the contributions to $k$ cut pomerons from diagrams with an arbitrary number of exchanged pomerons, then we get for $k > 1$ with the weights in ref [26] a Poisson distribution. For fixed impact parameter the assumptions in the `Pythia` model are thus in agreement with the AGK rules.

### *5.3. Relation $E_\perp - n_{\rm ch}$*

Although Field's tunes of the `Pythia` model give good fits to data, there are still problems. The relation between transverse energy and hadron multiplicity is not what has been expected. In the AGK paper a cut pomeron was expected to give a chain of hadrons between the remnants of the two colliding hadrons, and two cut pomerons should give two such chains and therefore doubled particle density. This is in contrast to the CDF data, where $E_\perp$ grows more than the multiplicity in multiple collision events.

The original AGK paper was published before QCD, and based on a multiperipheral model. However, also in QCD the DGLAP or BFKL dynamics gives color-connected chains of gluons. In the hadronization process the gluon exchange ought to give two triplet strings (or cluster chains) stretching between the projectile remnants, and in the spirit of AGK two cut pomerons should give four such triplet strings. Field's tunes seem instead to indicate some kind of color recombination which reduces the effective string length. (Similar recombinations have been studied by Ingelman and coworkers [27].)

In the `Pythia` model used by Field different possibilities for the color connection between the partons involved are studied. The most common parton subcollisions are $gg \to gg$, and as mentioned above this is expected to give two strings between the projectile remnants. Initial state radiation gives extra gluons, for which the color ordering agrees with the ordering in rapidity. Therefore these emissions do not increase the total string length very much, and as a consequence they increase $E_\perp$ more than they increase the hadron multiplicity.

From the experimental data it was noted in Ref. [14] that two subcollisions could not give doubled multiplicity, as expected from four strings as discussed above. It was therefore assumed that the second subcollision could give a just single double string connecting the two outgoing gluons. Another option was replacing the gluons by a $q\bar{q}$ pair, connected by a single triplet string. This reduces the multiplicity even further. A third possibility was to assume that color rearrangement caused the scattered gluons to fit in the color chains of the first collision, in such a way that the total string length was increased as little as possible. This gives a minimal additional

multiplicity, and in this case the multiple collisions have an effect on the total $E_\perp$ and multiplicity similar to the bremsstrahlung gluons (but the jets are balanced pairwise in transverse momentum). The default assumption in Ref. [14] was to give each of these possibilities the same probability, 1/3. In Field's successful tunes these ratios are changed, such that the last option with color reconnection is chosen in 90% of the cases.

In a more recent study by Sjöstrand and Skands [13] a number of improvements have been added to the old `Pythia` model. The hope was that with these modifications it would be possible to describe data without the extreme color reconnections which have no real theoretical motivation in QCD. Their result is, however, discouraging, as they were not able to tune the new model to give the relation between $p_\perp$ and multiplicity observed in the data.

## 6. Theoretical ideas

### *6.1. Pomeron interactions*

We have to conclude that something important is missing in our understanding of high energy collisions. Although, in the AGK paper, pomeron interactions are assumed to give small contributions, pomeron vertices (see *e.g.* [28]) and pomeron loops may be very important. As indicated in Fig. 5(a), a pomeron loop can give a bump in the particle density if both branches of the loop are cut, and a gap if the cut passes between the two branches. It is also conceivable that such gaps and bumps have to be included in a "renormalized" pomeron [29].

In QCD a pomeron is formed by two gluons in a color singlet. Two pomeron exchange thus corresponds to four gluons in two singlet pairs. If the pairs (1,2) and (3,4) form singlets, then gluon exchange can change the system so that instead the pairs (1,3) and (2,4) form color singlets. This corresponds to an effective $2I\!P \to 2I\!P$ coupling (*cf.* Ref. [30]). A cut with gluons 1 and 2 on one side and 3 and 4 on the other can then give an isolated bump in the particle density, as illustrated in Fig. 5(b). This type of pomeron interactions can also give a bound state [31], which gives a pole in the angular momentum plane and an essential correction to the normal cut from the exchange of two uncorrelated pomerons.

We conclude that there are still many open questions. More experimental information is needed, and to gain insight into the dynamics it is important to go beyond inclusive observables, and study observables related to correlations and fluctuations.

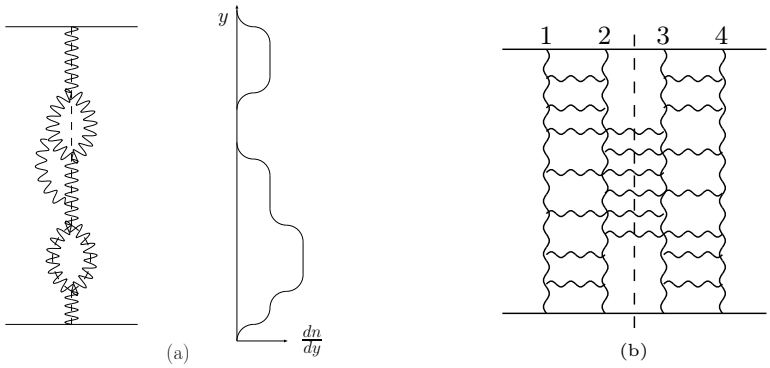


Fig. 5. (a) A pomeron loop can be cut through 0, 1, or 2 of its two branches. This can give gaps and bumps in the particle distribution. (b) Two pomerons can be represented by four gluons in two color singlet pairs. Gluon exchange can switch the pairs (1,2) (3,4) into the singlet pairs (1,3) (2,4). A cut as indicated in the figure gives a localized bump in the rapidity distribution.

### *6.2. Dipole cascade models, saturation and pomeron loops*

Multiple scattering and rescattering is more easily treated in transverse coordinate space. In Mueller's dipole cascade model [32, 33] a color dipole formed by a $q\bar{q}$ pair in a color singlet is split into two dipoles by gluon emission. Each of these dipoles can split repeatedly into a cascade, see Fig. 6(a). The probability per unit rapidity for a split is proportional to $\bar{\alpha} = N_c\alpha_s/\pi$. When two dipole chains collide, gluon exchange between two dipoles implies exchange of color and a recoupling of the chains, as shown in Fig. 6(b). The probability for an interaction between two dipoles $i$ and $j$, $f_{ij}$, is proportional to $\alpha_s^2 = \pi^2\bar{\alpha}^2/N_c^2$, and is thus formally color suppressed compared to the dipole splitting process.

In the eikonal approximation the total scattering probability is determined by the expression $1 - \prod_{ij}(1 - f_{ij})$, which is always smaller than 1 and thus satisfies the constraints from unitarity. As seen in Fig. 7(a), multiple dipole–dipole interactions can imply that the color dipoles form closed loops, which correspond to the pomeron loops in Fig. 5(a). Mueller's model includes those pomeron loops, which correspond to cuts in the particular Lorentz frame used for the calculation, but not loops which are fully inside one of the colliding cascades. This implies that the formalism is not Lorentz frame independent, and different ways have been suggested to achieve a frame independent formulation (see *e.g.* Refs. [34, 35]). However, so far no explicitely frame independent formalism has been presented.

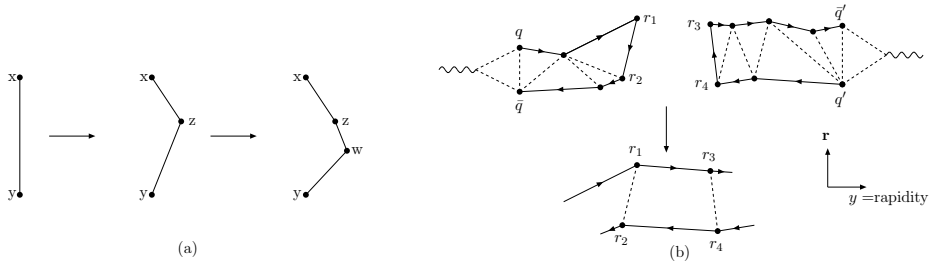


Fig. 6. (a) The evolution of the dipole cascade. At each step, a dipole can split into two new dipoles. (b) A symbolic picture of a $\gamma^*\gamma^*$ collision in $y - \boldsymbol{r}_\perp$-space. When two colliding dipoles interact via gluon exchange the color connection between the gluons is modified. The result is dipole chains stretched between the remnants of the colliding systems.

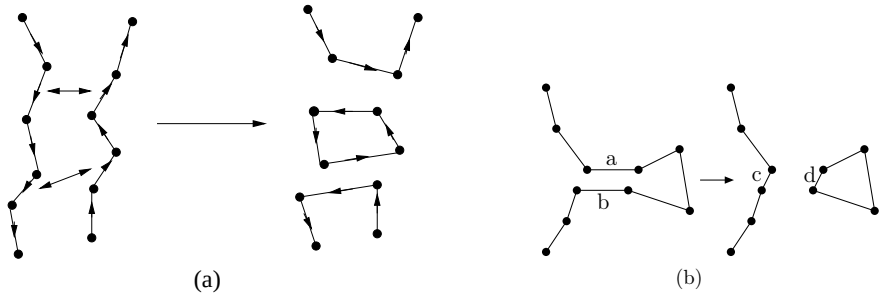


Fig. 7. (a) If more than one pair of dipoles interact it can result in dipole loops, which correspond to pomeron loops. (b) Schematic picture of a dipole swing. If the two dipoles $a$ and $b$ have the same color, they can be replaced by the dipoles $c$ and $d$. The result is a closed loop formed within an individual dipole cascade.

In one approach the evolution is expressed in terms of *interacting* dipoles. This implies that the number of dipoles can be reduced, and the evolution of the projectile cascade depends on the target. Besides the $1 \to 2$ dipole vertex there should here also be a $2 \to 1$ vertex. In another approach the evolution of the projectile is independent of the target, and the non-interacting dipoles are eliminated afterwards. In this approach there is no need to reduce the number of dipoles in the evolution.

*Dipole swing*

A model based on the latter approach is presented in Ref. [36]. In this model pomeron loops can be formed with the help of a recoupling of the dipole chains, a "dipole swing". Just as the dipole–dipole scattering, the pomeron loops in the cascades should be color suppressed. With a finite number of colors we can have not only dipoles but also higher color multi-

poles. Two charges and two anticharges with the same color may be better approximated by two dipoles formed by nearby charge–anticharge pairs. These pairs may be different from the initially generated dipoles, and the result is a recoupling of the dipole chain, as seen in Fig. 7(b). The same effect can also be obtained from gluon exchange, which is proportional to $\alpha_s$ and thus also color suppressed *cf.* to the dipole splitting proportional to $\bar{\alpha}$.

The swing does not result in a reduction of the number of dipoles, but the saturation effect is obtained as the recoupled dipoles are smaller and therefore have smaller cross-sections. Inserted in a MC the result is approximately frame independent, and the model describes well both the $F_2$ structure function in DIS and the $pp$ scattering cross section [36, 37], as shown in Fig. 8. (For these results also energy conservation and a running $\alpha_s$ are very important.) We see here that the $\gamma^* p$ cross-section satisfies geometric scaling. The $pp$ cross-section is reduced by about a factor 4 *cf.* to the one pomeron exchange at the Tevatron, and we also see that the result of the model is the same when calculated in the cms as in the rest frame of the target proton, if pomeron loops are included also in the evolution via the dipole swing.

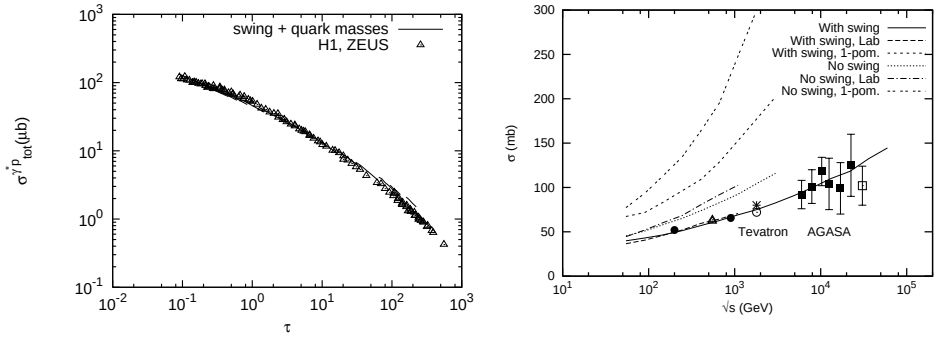


Fig. 8. Results from the dipole cascade model in Refs. [36, 37]. Left: The $\gamma p$ total cross-section plotted as a function of the scaling variable $\tau = Q^2/Q_s^2$, where $Q_s^2 = Q_0^2(x_0/x)^\lambda$ with $Q_0 = 1\text{GeV}$, $x_0 = 3 \times 10^{-4}$, $\lambda = 0.29$. Right: The total $pp$ scattering cross-section. Results are presented for evolution with and without the dipole swing mechanism. The one pomeron result and the result obtained in a frame where one of the protons is almost at rest are also shown.

Besides the total cross-sections it is also possible to calculate the probability to have pomeron loops formed by multiple collisions in a given frame, or loops formed within the cascades. As examples we find at the Tevatron in the cms on average 2.2 loops from multiple collisions and 0.65 loops in each of the two cascades. In an asymmetric frame, where the total rapidity range is divided in 4.5 + 10.5 units, we find instead 2 loops from multiple

collisions, and 0.15 and 1.35 in the two cascades, respectively. In both cases this gives in total 3.5 loops. At LHC we obtain in the same way in total an average of 5 loops.

Using the eikonal approximation it is besides total cross-sections also possible to calculate elastic scattering and diffractive excitation [38], but so far it has not been possible to calculate exclusive final states. The aim for the future is to bridge the gap between dipole cascades, AGK, and traditional MC generators, and construct an event generator fully compatible with unitarity and the AGK cutting rules.

## 7. Conclusions

• Experimental data are well described by a hadronization model based on a stringlike confining field, where gluons act as transverse excitations on the string. An important feature of the string model is the infrared stability.

• Parton cascade models based on leading $1/N_c$ expansion work well for timelike parton cascades in $e^+e^-$ annihilation. (Why is there no color reconnection?)

• Spacelike cascades are more complicated. There are two different problems: the cross-section and the final states. Non-$k_\perp$-ordered cascades are not fully understood.

• Multiple collisions are present in data, and the hard subcollisions are correlated. The underlying event is different from a minimum bias event.

• Rick Field's tunes of the `Pythia` MC fit Tevatron data well, but the relation between transverse energy and multiplicity is not understood. This may indicate some kind of color rearrangement, or a "renormalized pomeron".

• Multiple collisions and unitarity constraints are easier treated in transverse coordinate space. The dipole formalism can describe $I\!P$ loops and diffraction. The application of AGK cutting rules then implies the presence of rapidity gaps.

• For the future we hope to be able to combine the dipole formalism and traditional MC generators to obtain event generators which include diffraction and are compatible with unitarity and AGK.

## REFERENCES

[1] B. Andersson, G. Gustafson, G. Ingelman, T. Sjöstrand, *Phys. Rep.* **97**, 31 (1983).

[2] R. Duran Delgado, G. Gustafson, L. Lönnblad, *Eur. Phys. J.* **C52**, 113 (2007).

[3] T. Sjöstrand *et al.*, *Comput. Phys. Commun.* **135**, 238 (2001).

[4] [JADE Collaboration], *Phys. Lett.* **B157**, 340 (1985); *Z. Phys.* **C39**, 1 (1988).
[5] G. Marchesini *et al.*, *Comput. Phys. Commun.* **67**, 465 (1992).
[6] A. Bassetto *et al.*, *Phys. Rep.* **100** (1983) 201.
[7] G. Gustafson, U. Pettersson, *Nucl. Phys.* **B306**, 746 (1988).
[8] L. Lönnblad, *Comput. Phys. Commun.* **71**, 15 (1992) 15.
[9] P. Abreu *et al.* [DELPHI Collaboration], *Z. Phys.* **C73**, 11 (1996).
[10] M. Ciafaloni, *Nucl. Phys.* **B296**, 49 (1988); S. Catani *et al.*, *Phys. Lett.* **B234**, 339 (1990); *Nucl. Phys.* **B336**, 18 (1990).
[11] B. Andersson, G. Gustafson, J. Samuelsson, *Nucl. Phys.* **B467**, 443 (1996).
[12] B. Andersson *et al.*, *Z. Phys.* **C43**, 625 (1989).
[13] T. Sjöstrand, P.Z. Skands, *J. High Energy Phys.* **03**, 053 (2004).
[14] T. Sjöstrand, M. van Zijl, *Phys. Rev.* **D36**, 2019 (1987).
[15] G. Gustafson, L. Lönnblad, G. Miu, *Phys. Rev.* **D67**, 034020 (2003).
[16] D. Cline, F. Halzen, J. Luthe, *Phys. Rev. Lett.* **31**, 491 (1973).
[17] S.D. Ellis, M.B. Kislinger, *Phys. Rev.* **D9**, 2027 (1974).
[18] T. Akesson *et al.*, *Z. Phys.* **C34**, 163 (1987).
[19] F. Abe *et al.*, *Phys. Rev.* **D47**, 4857 (1993).
[20] V.M. Abazov *et al.*, *Phys. Rev.* **D67**, 052001 (2003).
[21] F. Abe *et al.*, *Phys. Rev.* **D56**, 3811 (1997).
[22] C. Gwenlan, *Acta Phys. Pol. B* **33**, 3123 (2002).
[23] C. Albajar *et al.*, *Nucl. Phys.* **B309**, 405 (1988).
[24] S. Aid et al., *Z. Phys.* **C70**, 17 (1996).
[25] R.D. Field, Contrib. to ICHEP 06, Moscow, Russia, 26 July–2 August 2006.
[26] V.A. Abramovsky, V.N. Gribov, O.V. Kancheli, *Yad. Fiz.* **18**, 595 (1973).
[27] R. Enberg, G. Ingelman, N. Timneanu, *Phys. Rev.* **D64**, 114015 (2001).
[28] J. Bartels, M. Wusthoff, *Z. Phys.* **C66**, 157 (1995).
[29] S. Ostapchenko, *Phys. Lett.* **B636**, 40 (2006).
[30] J. Bartels, M. Salvadore, G.P. Vacca, *Eur. Phys. J.* **C42**, 53 (2005).
[31] J. Bartels, M.G. Ryskin, *Z. Phys.* **C60**, 751 (1993); *Z. Phys.* **C62**, 425 (1994).
[32] A.H. Mueller, *Nucl. Phys.* **B415**, 373 (1994); *Nucl. Phys.* **B437** (1995) 107.
[33] A.H. Mueller, B. Patel, *Nucl. Phys.* **B425**, 471 (1994).
[34] E. Iancu, G. Soyez, D.N. Triantafyllopoulos, *Nucl. Phys.* **A768**, 194 (2006).
[35] M. Kozlov, E. Levin, A. Prygarin, *Nucl. Phys.* **A792**, 122 (2007).
[36] E. Avsar, G. Gustafson, L. Lönnblad, *J. High Energy Phys.* **07**, 062 (2005); *J. High Energy Phys.* **01**, 012 (2007).
[37] E. Avsar, G. Gustafson, *J.High Energy Phys.* **04**, 067 (2007).
[38] E. Avsar, G. Gustafson, L. Lönnblad, *J. High Energy Phys.* **0712**, 012 (2007).